

Transmit Beampattern Synthesis for Planar Array with One-bit DACs

Tong Wei, Linlong Wu, Mohammad Alae-Kerahroodi and Bhavani Shankar M. R.

Interdisciplinary Centre for Security, Reliability and Trust (SnT), University of Luxembourg
Luxembourg City, Luxembourg
email: {tong.wei, linlong.wu, mohammad.alae, bhavani.shankar}@uni.lu.

Abstract: *In this paper, the problem of transmit beampattern synthesis for planar array, which deploys one-bit digital-to-analog converters (DACs), is investigated. By properly designing the emitted signal quantized by one-bit DACs, the synthesized transmit beampattern is able to approximate a desired beampattern closely. However, the formulated problem is highly nonconvex due to the quartic objective and the discrete binary constraint. To tackle this problem, we first reformulate it into quadratic objective with interval constraint. On this basis, the alternating direction multiplier method (ADMM) framework is used to solve the resulting quadratic program (QP) problem. Simulation results will demonstrate the effectiveness of our method.*

1. Introduction

Multiple-input multiple-output (MIMO) radar system has attracted much research interest in the recent years [1], [2]. Compared with its phased-array counterpart, MIMO radar can offer significant enhancement in target detection [3]-[5] and flexibility of transmit beampattern synthesis [6]-[8]. Particularly, transmit beampattern can generally determine the intensity of backscattered signal and hence plays a vital role in MIMO radar [5]. Consequently, synthesizing the desired transmit beampattern under some predefined criteria becomes a crucial problem.

In general, the existing beampattern design methods can be classified into two categories. The first approach allocates an optimal weight for each transmitter known as weight-based method (i.e., transmit beamforming) [9]-[12]. For example, in [9], the problem of beampattern synthesis is first formulated as second-order cone program (SOCP) and semidefinite program (SDP) which are convex and can be solved by some commercial optimization tools. Meanwhile, the sparse array beampattern synthesis is considered in [10]-[12], can reach a preferable beampattern with a fewer number of elements. In this scenario, the nonconvex l_0 -norm minimization problem should be solved appropriately. In [12], the authors first utilize l_p -norm ($0 < p < 1$) to smoothly approximate the nonconvex l_0 -norm and then handle the norm minimization problem via the alternating direction method of multipliers (ADMM) algorithm. By doing so, the final solution achieves a good balance between objective value and sparsity.

The second category achieves the desired beampattern via direct waveform design [8], [13]-[17]. Since it can simultaneously design multiple non-orthogonal waveforms, this kind of

method is more suitable for MIMO radar. For example, in [8], the beampattern match error and the cross-correlation sidelobes are jointly minimized via designing the transmit waveform. The double-ADMM algorithm is devised to deal with the l_1 -norm minimization problem. The authors in [13] proposed a novel method to focus the transmit energy into the region(s) of interest via devising the cross-correlation matrix of emitted signal. Due to the exploitation of energy focusing, the proposed method shows improved target localization performance. After that, in [14], the constant modulus (CM) waveform is directly synthesized to achieve minimum peak sidelobe transmit beampattern. Different from the previous tasks, in [16], the coexistence problem between MIMO radar and MIMO communication system is addressed via designing the discrete-phase sequence.

It is worth noting that in the aforementioned schemes, high-resolution digital-to-analog converters (DACs) are considered by default. However, it will cause massive power consumption and huge hardware cost when employing MIMO radars, especially in a planar array configuration. This motivates the use of low resolution DACs. Recently, in [17], the low-resolution DACs is utilized to beampattern design. However, this method needs several time approximation which can lead some performance loss. In this paper, we aim to design the transmit beampattern for planar array which deploys one-bit DACs. Different from [17], we will directly solve the original problem and hence does not suffer from performance loss as in [17]. Finally, the resulting quadratic program (QP) problem can be solved efficiently within the ADMM framework. Simulation results will demonstrate the effectiveness of the proposed method.

2. Problem Formulation

2.1. System Model on Planar Array

Let us consider a rectangular planar array with $M \times N$ omnidirectional antennas, placed with the inter-element spacings d_x and d_y along x and y axes, respectively. Then, the input signal waveform matrix can be denoted as

$$\mathbf{S}(t) = \begin{pmatrix} s_{1,1}(t) & \cdots & s_{1,N}(t) \\ \vdots & \ddots & \vdots \\ s_{M,1}(t) & \cdots & s_{M,N}(t) \end{pmatrix}, \quad (1)$$

where $s_{m,n}(t)$ denotes the signal transmitted from the (m, n) -th antenna and $t = 1, \dots, T$ denotes the discrete time instances. To reduce the complexity of RF chain, in this paper, a pair of one-bit DACs are deployed to quantize the real and imaginary part of input signal, respectively. Therefore, the resulting one-bit signal waveform matrix is denoted as follows

$$\mathbf{X}(t) = \begin{pmatrix} x_{1,1}(t) & \cdots & x_{1,N}(t) \\ \vdots & \ddots & \vdots \\ x_{M,1}(t) & \cdots & x_{M,N}(t) \end{pmatrix}, \quad (2)$$

where $x_{m,n}(t) = \mathcal{Q}_c(s_{m,n}(t))$ and $\mathcal{Q}_c(\cdot) = \mathcal{Q}(\cdot) + j\mathcal{Q}(\cdot)$ denotes the complex-value one-bit quantizer [17]. Thus, we have

$$\mathcal{Q}(z) = \begin{cases} +\alpha, & z \geq 0 \\ -\alpha, & z < 0 \end{cases} \quad (3)$$

where α depends on the transmit power.

Without loss of generality, we assume that E_t is the total transmit power budget. Hence, we have

$$\sum_{t=1}^T \|\mathbf{X}(t)\|_2^2 = 2\alpha^2 MNT = E_t, \quad (4)$$

which means that $\alpha = \sqrt{\frac{E_t}{2MNT}}$ and $x_{m,n}(t) \in \{\pm\alpha \pm j\alpha\}$.

For the t -th time sample, the receive signal at azimuth angle θ and elevation angle ϕ can be written as

$$y(\theta, \phi, t) = \sum_{m=1}^M \sum_{n=1}^N x_{m,n}(t) e^{j\frac{2\pi}{\lambda}((m-1)d_x \sin \phi \cos \theta)} \cdot e^{j\frac{2\pi}{\lambda}((n-1)d_y \sin \phi \sin \theta)}, \quad (5)$$

where λ denotes the signal wavelength. Assuming $d_x = d_y = \frac{\lambda}{2}$, the (5) can be rewritten as

$$y(\mu_x, \mu_y, t) = \sum_{m=1}^M \sum_{n=1}^N x_{m,n}(t) e^{j\pi((m-1)\mu_x + (n-1)\mu_y)} = \mathbf{a}^T(\mu_x, \mu_y) \mathbf{x}(t), \quad (6)$$

where $\mu_x = \sin \phi \cos \theta$ and $\mu_y = \sin \phi \sin \theta$ denote the directional cosines, respectively, $\mathbf{x}(t) = \text{vec}(\mathbf{X}(t))$ and

$$\mathbf{a}(\mu_x, \mu_y) = \begin{bmatrix} 1 \\ e^{j\pi\mu_y} \\ \vdots \\ e^{j\pi(N-1)\mu_y} \end{bmatrix} \otimes \begin{bmatrix} 1 \\ e^{j\pi\mu_x} \\ \vdots \\ e^{j\pi(M-1)\mu_x} \end{bmatrix} \quad (7)$$

denotes the equivalent transmit steering vector. Noticed that the proposed method can be directly used to uniform linear array (ULA) via letting $\theta = 0^\circ$ or replacing the above steering vector as $\mathbf{a}(\theta) = [1, e^{j\pi \sin \phi}, \dots, e^{j\pi(M-1) \sin \phi}]$.

Following above expressions, the transmit beampattern, which characterizes the spatial power spectrum, is given by

$$\begin{aligned} P(\mu_x, \mu_y) &= \sum_{t=1}^T \mathbf{x}(t)^H \mathbf{a}^*(\mu_x, \mu_y) \mathbf{a}^T(\mu_x, \mu_y) \mathbf{x}(t) \\ &= \mathbf{x}^H (\mathbf{I}_T \otimes \mathbf{a}^*(\mu_x, \mu_y) \mathbf{a}^T(\mu_x, \mu_y)) \mathbf{x} \\ &= \mathbf{x}^H \mathbf{A}(\mu_x, \mu_y) \mathbf{x}, \end{aligned} \quad (8)$$

where $\mathbf{x} = [\text{vec}^T(\mathbf{X}(1)), \dots, \text{vec}^T(\mathbf{X}(T))]^T$ denotes the completed signal sequence,

$$\mathbf{A}(\mu_x, \mu_y) = \mathbf{I}_T \otimes \mathbf{a}^*(\mu_x, \mu_y) \mathbf{a}^T(\mu_x, \mu_y) \quad (9)$$

is a diagonal block-sparse matrix and $(\cdot)^*$ denotes the complex conjugate.

2.2. Optimization Problem Formulation

Firstly, the desired grid of the transmit beampattern can be denoted as

$$\{\mu_{x,l}, \mu_{y,k}\} \in \mathcal{U}, l=1, \dots, L, k=1, \dots, K, \quad (10)$$

where \mathcal{U} denotes the total grid of completed beampattern region, and L and K are the number of the discrete points along x and y axes, respectively. According to the beampattern matching criteria, we plan to minimize the following objective function

$$J(\gamma, \mathbf{x}) = \sum_{l=1}^L \sum_{k=1}^K |P(\mu_{x,l}, \mu_{y,k}) - \gamma d(\mu_{x,l}, \mu_{y,k})|^2 = \sum_{l=1}^L \sum_{k=1}^K |\mathbf{x}^H \mathbf{A}(\mu_{x,l}, \mu_{y,k}) \mathbf{x} - \gamma d(\mu_{x,l}, \mu_{y,k})|^2, \quad (11)$$

where $\gamma > 0$ is a scaling factor and $d(\mu_{x,l}, \mu_{y,k})$ denotes the desired beampattern. Towards obtaining simplified notation, $\mathbf{A}(\mu_{x,l}, \mu_{y,k})$ and $d(\mu_{x,l}, \mu_{y,k})$ will be denoted by $\mathbf{A}(l, k)$ and $d(l, k)$, respectively, in the sequel.

Hereafter, we focus on designing the transmit signal sequence \mathbf{x} to match the desired beampattern. Mathematically, the following optimization problem can be formulated

$$\begin{aligned} \min_{\gamma, \mathbf{x}} \quad & J(\gamma, \mathbf{x}) = \sum_{l=1}^L \sum_{k=1}^K |\mathbf{x}^H \mathbf{A}(l, k) \mathbf{x} - \gamma d(l, k)|^2 \\ \text{s.t.} \quad & \mathbf{x} \in \mathcal{X}, \end{aligned} \quad (12)$$

where $\mathcal{X} = \{\pm\alpha \pm j\alpha\}^{MNT}$ denotes the corresponding feasible set of \mathbf{x} .

For the convenience of manipulations, the problem (12) can be converted to the corresponding real-value form

$$\begin{aligned} \min_{\gamma, \mathbf{x}_r} \quad & J(\gamma, \mathbf{x}_r) = \sum_{l=1}^L \sum_{k=1}^K |\mathbf{x}_r^T \mathbf{A}_r(l, k) \mathbf{x}_r - \gamma d(l, k)|^2 \\ \text{s.t.} \quad & \mathbf{x}_r \in \mathcal{X}_r, \end{aligned} \quad (13)$$

where $\mathcal{X}_r = \{\pm\alpha\}^{2MNT}$, $\mathbf{x}_r = [\Re\{\mathbf{x}\}^T, \Im\{\mathbf{x}\}^T]^T$ and

$$\mathbf{A}_r(l, k) = \begin{bmatrix} \Re\{\mathbf{A}(l, k)\} & -\Im\{\mathbf{A}(l, k)\} \\ \Im\{\mathbf{A}(l, k)\} & \Re\{\mathbf{A}(l, k)\} \end{bmatrix}. \quad (14)$$

It is noticed that the problem (13), which involves in fourth-order objective function and discrete binary constraint, is difficult to solve directly. Hence, we will introduce a novel method to tackle this nonconvex problem based on the ADMM framework.

3. ADMM-Based Algorithm

To begin with, let us introduce an important variable reformulation.

Proposition 1. *If we define set $\Upsilon \triangleq \{(\mathbf{x}_r, \mathbf{v}) \mid \mathbf{x}_r - \mathbf{v} = \mathbf{0}, \|\mathbf{v}\|_\infty \leq \sqrt{\frac{E_t}{2MNT}}, \|\mathbf{x}_r\|_2^2 = E_t\}$ and assume that $(\mathbf{x}_r, \mathbf{v}) \in \Upsilon$, then we immediately conclude that both \mathbf{v} and $\mathbf{x}_r \in \mathcal{X}_r$.*

Proof. The proof is simple and can be obtained in [18]. □

Based on above, problem (13) can be equivalently reformulated as

$$\begin{aligned} \min_{\gamma, \mathbf{x}_r, \mathbf{v}} \quad & J(\gamma, \mathbf{x}_r, \mathbf{v}) = \sum_{l=1}^L \sum_{k=1}^K |\mathbf{x}_r^T \mathbf{A}_r(l, k) \mathbf{v} - \gamma d(l, k)|^2 \\ \text{s.t.} \quad & \mathbf{x}_r - \mathbf{v} = \mathbf{0} \\ & \|\mathbf{x}_r\|_2^2 = E_t \\ & -\alpha \leq v_i \leq +\alpha, i=1, \dots, 2MNL \end{aligned} \quad (15)$$

where v_i denotes the i -th entry of \mathbf{v} .

The augmented Lagrangian function of problem (15) is given by

$$\mathcal{L}(\gamma, \mathbf{x}_r, \mathbf{v}, \mathbf{e}, \rho) = J(\gamma, \mathbf{x}_r, \mathbf{v}) + \mathbf{e}^T (\mathbf{x}_r - \mathbf{v}) + \frac{\rho}{2} \|\mathbf{x}_r - \mathbf{v}\|_2^2, \quad (16)$$

where \mathbf{e} is the Lagrangian multiplier vector, $\rho > 0$ denotes the penalty parameter. Within the framework of ADMM, the $(t+1)$ -th update procedure for problem (15) is given by

$$\gamma^{(t+1)} = \underset{\gamma}{\operatorname{argmin}} \mathcal{L}(\gamma, \mathbf{x}_r^{(t)}, \mathbf{v}^{(t)}, \mathbf{e}^{(t)}, \rho), \quad (17a)$$

$$\mathbf{x}_r^{(t+1)} = \underset{\|\mathbf{x}_r\|_2^2 = E_t}{\operatorname{argmin}} \mathcal{L}(\gamma^{(t+1)}, \mathbf{x}_r, \mathbf{v}^{(t)}, \mathbf{e}^{(t)}, \rho), \quad (17b)$$

$$\mathbf{v}^{(t+1)} = \underset{v_i \in \mathcal{D}}{\operatorname{argmin}} \mathcal{L}(\gamma^{(t+1)}, \mathbf{x}_r^{(t+1)}, \mathbf{v}, \mathbf{e}^{(t)}, \rho), \quad (17c)$$

$$\mathbf{e}^{(t+1)} = \mathbf{e}^{(t)} + \rho(\mathbf{x}_r^{(t+1)} - \mathbf{v}^{(t+1)}). \quad (17d)$$

In the following, we shall discuss in detail how to solve the optimization problems (17a)-(17d).

3.1. Update of γ

For the $(t+1)$ -th iteration, if we fix the variable vector $\{\mathbf{x}_r^{(t)}, \mathbf{v}^{(t)}, \mathbf{e}^{(t)}\}$, the parameter γ can be updated by solving the following unconstrained problem

$$\min_{\gamma} J(\gamma, \mathbf{x}_r^{(t)}, \mathbf{v}^{(t)}), \quad (18)$$

whose closed-form solution can be directly derived and given by

$$\gamma^{(t+1)} = \frac{\sum_{l=1}^L \sum_{k=1}^K d(l, k) \mathbf{x}_r^{(t)T} \mathbf{A}_r(l, k) \mathbf{v}^{(t)}}{\sum_{l=1}^L \sum_{k=1}^K d^2(l, k)}. \quad (19)$$

Noted that the factor $\gamma^{(t+1)} > 0$ is always satisfied due to the constraint $\mathbf{x}_r^{(t)} = \mathbf{v}^{(t)}$.

3.2. Update of \mathbf{x}_r

If we fix the value of $\{\gamma^{(t+1)}, \mathbf{v}^{(t)}, \mathbf{e}^{(t)}\}$, the primal variable \mathbf{x}_r can be updated by solving the following problem

$$\begin{aligned} \min_{\mathbf{x}_r} \quad & \mathcal{L}(\gamma^{(t+1)}, \mathbf{x}_r, \mathbf{v}^{(t)}, \mathbf{e}^{(t)}, \rho) \\ \text{s.t.} \quad & \|\mathbf{x}_r\|_2^2 = E_t. \end{aligned} \quad (20)$$

Setting the first-order derivation of the objective of problem (20) to zero with respect to \mathbf{x}_r , we have

$$\sum_{l=1}^L \sum_{k=1}^K 2(\mathbf{A}_r(l, k) \mathbf{v}^{(t)} \mathbf{v}^{(t)T} \mathbf{A}_r^T(l, k) \mathbf{x}_r - \gamma^{(t+1)} \cdot d(l, k) \mathbf{A}_r(l, k) \mathbf{v}^{(t)}) + \mathbf{e}^{(t)} + \rho(\mathbf{x}_r - \mathbf{v}^{(t)}) = \mathbf{0}. \quad (21)$$

Hence, it is easily derived that

$$\begin{aligned} \hat{\mathbf{x}}_r^{(t+1)} = & \left\{ \sum_{l=1}^L \sum_{k=1}^K 2\mathbf{A}_r(l, k) \mathbf{v}^{(t)} \mathbf{v}^{(t)T} \mathbf{A}_r^T(l, k) + \rho \mathbf{I}_{2MNL} \right\}^{-1} \\ & \cdot \left\{ \sum_{l=1}^L \sum_{k=1}^K 2\gamma^{(t+1)} d(l, k) \mathbf{A}_r(l, k) \mathbf{v}^{(t)} + \rho \mathbf{v}^{(t)} - \mathbf{e}^{(t)} \right\}. \end{aligned} \quad (22)$$

Recalling the total power constraint, we can finally update

$$\mathbf{x}_r^{(t+1)} = \sqrt{E_t} \frac{\hat{\mathbf{x}}_r^{(t+1)}}{\|\hat{\mathbf{x}}_r^{(t+1)}\|_2}. \quad (23)$$

3.3. Update of \mathbf{v}

If we fix the value of $\{\gamma^{(t+1)}, \mathbf{x}_r^{(t+1)}, \mathbf{e}^{(t)}\}$, the primal variable \mathbf{v} can be updated by solving the following problem

$$\begin{aligned} \min_{\mathbf{v}} \quad & \mathcal{L}(\gamma^{(t+1)}, \mathbf{x}_r^{(t+1)}, \mathbf{v}, \mathbf{e}^{(t)}, \rho) \\ \text{s.t.} \quad & -\alpha \leq v_i \leq +\alpha, i = 1, \dots, 2MNL. \end{aligned} \quad (24)$$

Similarly, recalling the first-order optimal condition of problem (24) to zero with respect to \mathbf{v} , we have

$$\sum_{l=1}^L \sum_{k=1}^K 2(\mathbf{A}_r^T(l, k) \mathbf{x}_r^{(t+1)} \mathbf{x}_r^{(t+1)T} \mathbf{A}_r(l, k) \mathbf{v} - \gamma^{(t+1)} \cdot d(l, k) \mathbf{A}_r^T(l, k) \mathbf{x}_r^{(t+1)}) - \mathbf{e}^{(t)} + \rho(\mathbf{v} - \mathbf{x}_r^{(t+1)}) = \mathbf{0}. \quad (25)$$

Then, we obtain

$$\begin{aligned} \hat{\mathbf{v}}^{(t+1)} = & \left\{ \sum_{l=1}^L \sum_{k=1}^K 2\mathbf{A}_r^T(l, k) \mathbf{x}_r^{(t+1)} \mathbf{x}_r^{(t+1)T} \mathbf{A}_r(l, k) + \rho \mathbf{I} \right\}^{-1} \\ & \cdot \left\{ \sum_{l=1}^L \sum_{k=1}^K 2\gamma^{(t+1)} d(l, k) \mathbf{A}_r^T(l, k) \mathbf{x}_r^{(t+1)} + \rho \mathbf{x}_r^{(t+1)} + \mathbf{e}^{(t)} \right\}. \end{aligned} \quad (26)$$

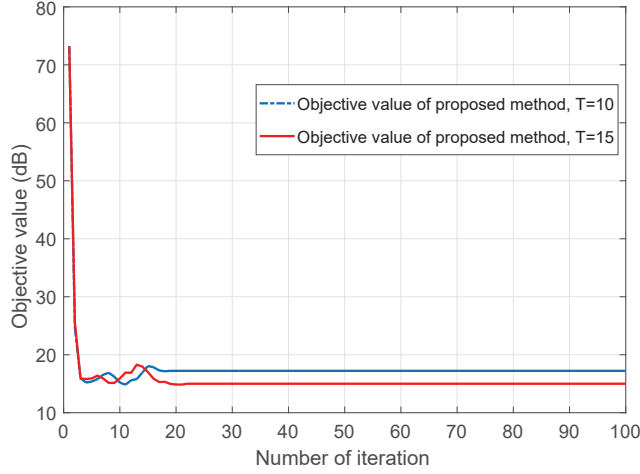


Figure 1: The objective value versus number of iteration.

According to the constraint of problem (24), it is immediately derived that

$$\mathbf{v}^{(t+1)} = \Pi_{\mathcal{D}}(\hat{\mathbf{v}}^{(t+1)}). \quad (27)$$

where $\Pi_{\mathcal{D}}(\cdot)$ denotes the element-wise projection operator onto set $\mathcal{D} = [-\alpha, +\alpha]$.

3.4. Update of \mathbf{e}

If the value of $\{\mathbf{x}_r^{(t+1)}, \mathbf{v}^{(t+1)}\}$ is fixed from previous update, the dual variable \mathbf{e} can be directly updated as follows

$$\mathbf{e}^{(t+1)} = \mathbf{e}^{(t)} + \rho(\mathbf{x}_r^{(t+1)} - \mathbf{v}^{(t+1)}). \quad (28)$$

4. Simulation Results

4.1. Linear Array Beampattern Synthesis

In this subsection, we demonstrate that the proposed algorithm can still be applied efficiently on the ULA case. The transmitter is composed of 12-element ULA with half-wavelength inter-element spacing. The whole spatial domain, i.e., $\phi \in [-90^\circ, 90^\circ]$, is uniformly sampled with a step-size of 1° . The region of interest is $\phi_m \in [-10^\circ, 10^\circ]$, where the desired pattern is $d(\phi_m) = 1000$. Without loss the generality, the total transmit power is fixed as $E_t = 1$. Meanwhile, the penalty parameter is set as $\rho^{(0)} = 10$ and a scaling factor of $\sigma = 1.2$ is used to scale it in each iteration. The initialization $(\mathbf{x}_r^{(0)}, \mathbf{v}^{(0)})$ is generated from a normal distribution with appropriate scaling to meet the total power E_t . Finally, we set $\mathbf{e}^{(0)} = \mathbf{0}$ and the maximum number of iteration is 100.

Fig. 1 demonstrates the value of objective function versus number of iterations for the proposed method. It is clear that our method can achieve good convergence performance for different time sample number (i.e., converge with around 30 times iteration). Meanwhile, the designed transmit signal waveform \mathbf{x}_r is perfectly one-bit sequence, which is consistent to our analysis. Fig. 2

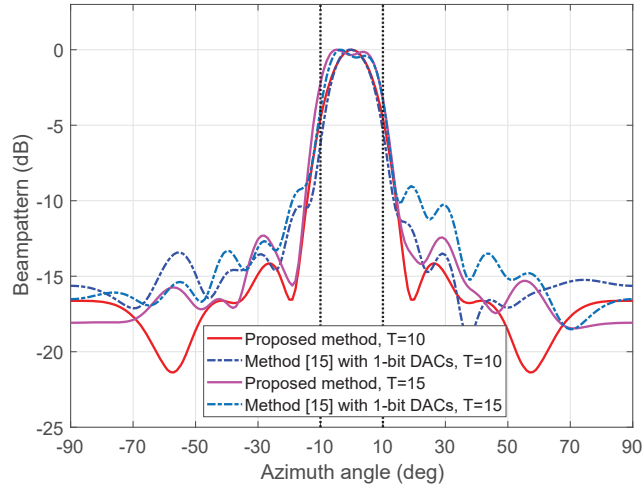


Figure 2: Comparison of transmit beampatterns with different time sample.

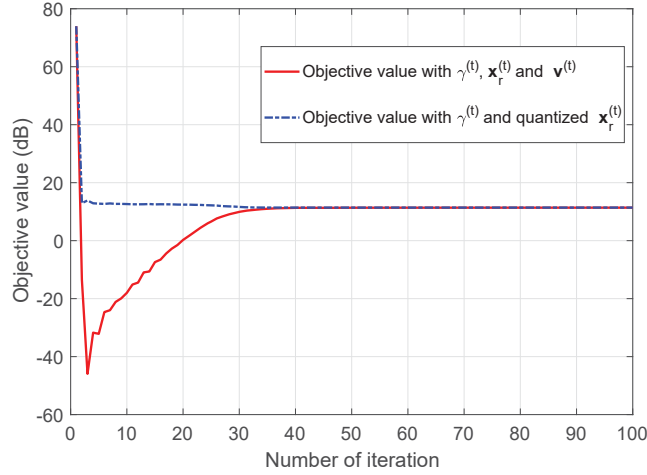


Figure 3: The objective value versus number of iteration.

displays the normalized transmit beampatterns for different methods. Obviously, the proposed method approximates the desired pattern more closely and has a lower sidelobe compared with method [15].

4.2. Planar Array Beampattern Synthesis

In this subsection, the transmitter is composed of a 5×5 element planer array with the inter-element spacings d_x and d_y equal to half-wavelength. We uniformly sample the directional cosines $\mu_x \in [-1, 1]$ and $\mu_y \in [-1, 1]$ with 0.05 step-size. The region of interest is set as $-0.25 \leq \tilde{\mu}_x \leq 0.25$ and $-0.25 \leq \tilde{\mu}_y \leq 0.25$, where the desired pattern $d(\tilde{\mu}_x, \tilde{\mu}_y) = 1000 \cdot |\cos(2\pi\tilde{\mu}_x) \cos(2\pi\tilde{\mu}_y)|$. All of the other parameters are set as same as previous section.

Fig. 3 shows the value of objective function versus number of iterations for the proposed method. The blue curve shows that the convergence plot for the quantized \mathbf{x}_r , i.e., $\mathcal{Q}(\mathbf{x}_r)$ at each ADMM iteration. It is interesting to note that the red curve indirectly reveals the inner

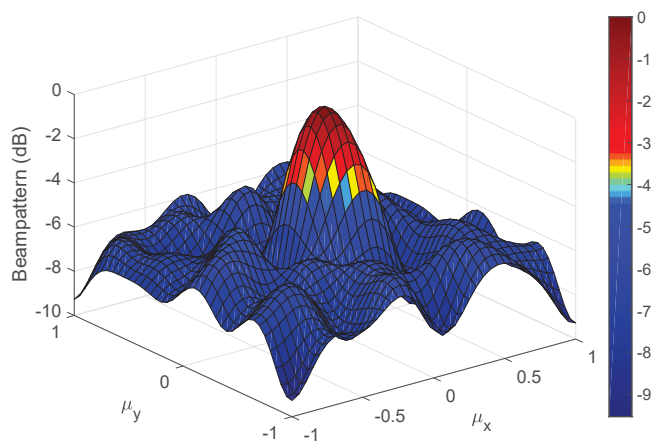


Figure 4: 3D view of transmit beampattern.

mechanism of ADMM. As the beginning stage, due to the larger feasible set, the objective value can be lower. But as the iteration goes, \mathbf{x}_r and \mathbf{v} are approaching each other, which means that \mathbf{x}_r is shifting from a good point to meet the one-bit constraint. Once again, it is seen that the transmit signal of proposed method can perfectly converge to one-bit sequence. Fig. 4 expresses the synthesized transmit beampattern for the planar array. It is seen that the majority emitted power can be focused on the region of interest. At the same time, the sidelobe level is also well controlled.

5. Conclusion

In this paper, a novel transmit beampattern synthesis algorithm for planar array with one-bit DACs is proposed. With the properly designed one-bit transmit waveform sequence, the synthesized beampattern can approach a desired pattern closely. To deal with the optimization problem, the fourth-order objective and discrete constraint are reformulated into the second-order objective and interval constraint, respectively. Meanwhile, the ADMM-based algorithm is developed to solve the resulting QP problem. The effectiveness of proposed method can be verified by simulation results. Finally, comparison with other works dealing with discrete alphabet design, we will extend our method to large-scale planar array scenario in the future work.

Acknowledgement

This work was supported by the Luxembourg National Research Fund (FNR) through the CORE project “SPRINGER” under Grant R-STR-5010-00-B/SPRINGER.

References

- [1] J. Li and P. Stoica, “MIMO radar with colocated antennas”, *IEEE Signal Processing Magazine*, Sept. 2007, vol. 24, no. 5, pp. 106-114.

- [2] A. M. Haimovich, R. S. Blum and L. J. Cimini, "MIMO radar with widely separated antennas", *IEEE Signal Processing Magazine*, 2008, vol. 25, no. 1, pp. 116-129.
- [3] I. Bekkerman and J. Tabrikian, "Target detection and localization using MIMO radars and sonars", *IEEE Transactions on Signal Processing*, Oct. 2006, vol. 54, no. 10, pp. 3873-3883.
- [4] J. Li, P. Stoica, L. Xu and W. Roberts, "On parameter identifiability of MIMO radar", *IEEE Signal Processing Letters*, Dec. 2007, vol. 14, no. 12, pp. 968-971.
- [5] A. Hassanien and S. A. Vorobyov, "Transmit energy focusing for DOA estimation in MIMO radar with colocated antennas", *IEEE Transactions on Signal Processing*, June 2011, vol. 59, no. 6, pp. 2669-2682.
- [6] P. Stoica, J. Li and Y. Xie, "On probing signal design for MIMO radar", *IEEE Transactions on Signal Processing*, Aug. 2007, vol. 55, no. 8, pp. 4151-4161.
- [7] P. Stoica, J. Li and X. Zhu, "Waveform synthesis for diversity-based transmit beampattern design", *IEEE Transactions on Signal Processing*, June 2008, vol. 56, no. 6, pp. 2593-2598.
- [8] Z. Cheng, Z. He, S. Zhang and J. Li, "Constant modulus waveform design for MIMO radar transmit beampattern", *IEEE Transactions on Signal Processing*, Sept. 2017, vol. 65, no. 18, pp. 4912-4923.
- [9] F. Wang, V. Balakrishnan, P. Y. Zhou, J. J. Chen, R. Yang and C. Frank, "Optimal array pattern synthesis using semidefinite programming", *IEEE Transactions on Signal Processing*, May 2003, vol. 51, no. 5, pp. 1172-1183.
- [10] B. Fuchs, "Synthesis of sparse arrays with focused or shaped beampattern via sequential convex optimizations", *IEEE Transactions on Antennas and Propagation*, July 2012, vol. 60, no. 7, pp. 3499-3503.
- [11] S. E. Nai, W. Ser, Z. L. Yu and H. Chen, "Beampattern synthesis for linear and planar arrays with antenna selection by convex optimization", *IEEE Transactions on Antennas and Propagation*, Dec. 2010, vol. 58, no. 12, pp. 3923-3930.
- [12] J. Liang, X. Zhang, H. C. So and D. Zhou, "Sparse array beampattern synthesis via alternating direction method of multipliers", *IEEE Transactions on Antennas and Propagation*, May 2018, vol. 66, no. 5, pp. 2333-2345.
- [13] T. Wei, H. Huang and B. Liao, "MIMO radar transmit beampattern synthesis via waveform design for target localization", *IEEE International Conference on Acoustics, Speech and Signal Processing (ICASSP)*, May, 2019, pp. 4285-4289.
- [14] W. Fan, J. Liang and J. Li, "Constant modulus MIMO radar waveform design with minimum peak sidelobe transmit beampattern", *IEEE Transactions on Signal Processing*, Aug. 2018, vol. 66, no. 16, pp. 4207-4222.
- [15] Z. Cheng, C. Han, B. Liao, Z. He and J. Li, "Communication-aware waveform design for MIMO radar with good transmit beampattern", *IEEE Transactions on Signal Processing*, Nov. 2018, vol. 66, no. 21, pp. 5549-5562.
- [16] M. Alae-Kerahroodi, K. V. Mishra, M. R. Bhavani Shankar and B. Ottersten, "Discrete-phase sequence design for coexistence of MIMO radar and MIMO communications", *IEEE 20th International Workshop on Signal Processing Advances in Wireless Communications (SPAWC)*, July, 2019, pp. 1-5.
- [17] Z. Cheng, B. Liao, Z. He and J. Li, "Transmit signal design for large-scale MIMO system with 1-bit DACs", *IEEE Transactions on Wireless Communications*, Sept. 2019, vol. 18, no. 9, pp. 4466-4478.
- [18] G. Yuan and B. Ghanem, "Binary optimization via mathematical programming with equilibrium constraints", *arXiv preprint:1608.04425*, Sept. 2016.